

Toshiaki Kozu<sup>\*1</sup>, K. Krishna Reddy<sup>2</sup>, Toyoshi Shimomai<sup>1</sup>, Hiroyuki Hashiguchi<sup>3</sup>, G. Viswanathan<sup>4</sup>  
<sup>1</sup> Shimane University, Matsue, Japan, <sup>2</sup> FORSGC, Yokosuka, Japan, <sup>3</sup> RASC/Kyoto University, Uji, Japan,  
<sup>4</sup> ISRO/ISTRAC, Bangalore, India

## 1. INTRODUCTION

Raindrop size distribution (DSD) is among the most fundamental rain parameters for quantitative radar rainfall remote sensing. Since mid 1980's, atmospheric sounding Doppler radars have been recognized as a useful tool to estimate vertical DSD profiles to study microphysical processes of precipitation and to develop DSD models for spaceborne rain radar algorithms.

In this presentation, we show preliminary results of vertical DSD profiles estimated from the data obtained from the Indian MST radar and the Lower Atmospheric Wind Profiler (LAWP) (Reddy *et al.*, 2002), Gadanki, south India, and the Equatorial Atmosphere Radar (EAR) developed jointly by RASC, Kyoto University and LAPAN, Indonesia (Fukao *et al.*, 2002) to study the DSD properties of tropical precipitation. The methodology of DSD estimation is a non-linear least square-based parametric estimation that have been employed by many researchers (e.g. Wakasugi *et al.*, 1987; Gossard, 1988). To improve the convergence performance in the iteration for the least-square estimation algorithm, we adopt a new parameterization of gamma DSD model, the superiority of which has been confirmed by computer simulations (Kozu *et al.*, 1998). The outline of the DSD parameterization and estimation method is also introduced.

## 2. Observation sites and instruments

Table 1 lists the location and observation systems at Gadanki, south India, and Koto Tabang, west Sumatra. The former site is located in the Indian monsoon climate, and relatively dry. The latter is located just on the equator and in Asian monsoon climate, hot and humid, and precipitation is much affected by local topography as well as large-scale climate systems.

<sup>\*</sup> Corresponding author address: Toshiaki Kozu, Shimane University, Matsue, Shimane 690-8504, Japan. e-mail: kozu@ecs.shimane-u.ac.jp

Table 1(a). Location of observation sites.

Gadanki	N13.47°, E79.10°, H 165 m, ASL
Koto Tabang	S0.20°, E100.32°, H 850 m, ASL

Table 1(b). Instruments at Gadanki.

Instruments	Description
Indian MST Radar	
Frequency	53 MHz
Antenna aperture	130 m x 130 m
Antenna beamwidth	3 deg.
Transmit power	2 MW
Range resolution	150 m
Probing altitudes	3 to 100 km
LAWP	
Frequency	1.357 GHz
Antenna aperture	4 m x 4 m
Antenna beamwidth	4 deg.
Transmit power	1 kW
Range resolution	75 m/150 m/300 m
Probing altitudes	up to 3-4 km
Others	
Disdrometer	RD-69
Rain gauge	ORG-815

Table 1(c). Instruments at Koto Tabang.

Instruments	Description
EAR	
Frequency	47 MHz
Antenna aperture	110 m x 110 m
Antenna beamwidth	3.4 deg.
Transmit power	100 kW
Range resolution	150 m
Others	
X-band rain radar	JMA-177 (JRC)
Disdrometer,	2DVD, RD-69 (*1)
Rain gauge	ORG-815, MAWS (*1)
WV profiler	WVP-1500
Micro-rain radar	MRR-2 (*2)

\*1 Operated by FORSGC. \*2 ILTS/Hokkaido University

## 3. DSD model parameterization

We assume the gamma DSD model that is usually represented by the three parameters ( $N_0$ ,  $L$  and  $m$ ):

$$N(D) = N_0 D^m e^{-LD}. \quad (1)$$

When we consider that the Doppler spectrum is proportional to  $D^6 |dv(D)/dD|^{-1}$  where  $D$  is the drop diameter,  $v(D)$  is the terminal velocity, the fitting of the Doppler spectrum can be made effectively by using a DSD parameter having a high sensitivity to the Doppler spectrum. Letting  $M_x$  be the  $x$ -th moment of DSD, and the DSD be modeled by a gamma

function,  $M_x$  is given by

$$M_x = N_0 G(\mathbf{m} + x + 1) / L^{\mathbf{m} + x + 1} \quad (2)$$

Choosing two arbitrary moments,  $M_x$  and  $M_y$ , the gamma DSD model can be expressed as follows:

$$N(D) = m_y L_{xy}^{\mathbf{m} + y + 1} D^{\mathbf{m}} e^{-L_{xy} D} \quad (3)$$

where  $m_y = M_y / G(\mathbf{m} + y + 1)$  and  $L_{xy} = (m_x / m_y)^{1/(y-x)}$ . In summary, we use Eq.3, i.e. DSD parameters of  $(m_y, L_{xy}, \mathbf{m})$  with  $x = 3.67$  and  $y = 6$ .

#### 4. Doppler spectrum model

As is usually done (Sato *et al.*, 1990), turbulence spectrum  $S_t(v)$  is modeled as a Gaussian function:

$$S_t(v) = p_0 \exp\left(-\frac{(v-w)^2}{2s^2}\right) \quad (4)$$

where  $p_0$  is the peak spectral power, and  $w$  and  $s$  are the mean and standard deviation. The precipitation spectrum  $S_p(v)$  is expressed as

$$S_p(v) = CN(D) D^6 |dv/dD|^{-1}. \quad (5)$$

Letting  $S_0(v)$  be the turbulence spectrum normalized to have a total power of unity, the entire Doppler spectrum (without fading noise)  $S(v)$  is given by

$$S(v) = S_t(v) + S_p(v) * S_0(v) + P_n \quad (6)$$

where  $P_n$  is the spectral noise power assumed to be constant over the spectral region. We estimate the seven unknown parameters, i.e.,  $p_0, w, s, P_n, m_y, L_{xy}$  and  $\mathbf{m}$  with a least-square criterion.

#### 5. Non-linear least square fitting

To estimate the seven unknown parameters, first we use the Marquardt method to estimate 6 parameters by fixing  $\mathbf{m}$ . Since it was reported that including  $\mathbf{m}$  as one of the unknown parameters in the non-linear least-square fitting can degrade the accuracy of other parameter estimation (Sato *et al.* 1990),  $\mathbf{m}$  is estimated in the second step by changing  $\mathbf{m}$  step-by-step, and choose the "best"  $\mathbf{m}$  that gives the minimum RMS error. The fitting is made in a log space to extend the dynamic range as was adopted by Sato *et al.* (1990); however, it is found from the simulation using this scheme can generate noticeable bias errors in higher-order DSD moment estimates. To reduce this problem, we adopt a "non-uniform weighting" in the least-square fitting in which heavier weights are given to higher spectral power region and turbulence spectrum region. This weighting sometimes degrades the fitting stability, however, and not so useful when precipitation echo power is relatively weak.

## 6. Some event analyses

### 6.1 Light-rain DSD estimation with LAWP

L-band radar is very sensitive to rain and it can be used for the DSD estimation only when rain is extremely light (around 0.1 mm/h or less). This may be useful to study microphysics in drizzle. Fig.1 shows examples of LAWP measured Doppler spectra and its fitting results. At low altitude, the turbulence spectrum is sufficiently large to estimate the turbulence parameters (Fig.1(a)); however, as altitude becomes higher, it becomes too weak to properly estimate the parameters (Fig.1(b)). This problem can partly be solved by using the weighted least-square method (Fig.1(c)).

In this event, turbulence spectra are detected only at limited altitudes, and DSD profiling is possible "partly".  $Z, R, L_{xy}$  and  $\mathbf{m}$  profiles as estimated from this method are shown in Fig.2. It should be noted that the decrease in  $Z$  and  $R$  below about 1.5 km might be caused by the saturation of the LAWP receiver. The radar calibration is made by adjusting LAWP reflectivities around 1.5 km with disdrometer-derived ones several minutes' after the LAWP observation. From Fig.2, we notice some systematic change in  $\mathbf{m}$  with height, suggesting raindrop break-up and/or evaporation of with decreasing height. It is necessary, however, to further evaluate the accuracy of DSD parameters when turbulence echo power is very weak as is shown in Fig.1(b,c).

### 6.2 DSD estimation with Indian MST radar

Although the VHF radar can be used for much higher rain rate than the L-band radar such as LAWP, a disadvantage is that it takes longer time to increase the number of independent samples ( $N_{inc}$ ) than in the L-band radar. In the present analysis, we obtain  $N_{inc} = 24$  with temporal and spectral averaging.

Fig.3 shows an example of measured and fitted Doppler spectrum at the height of 3.5 km. It is found that the non-uniform weighting improves the fitting of precipitation spectrum and neglects the turbulence spectral peak around 2 m/s. In cases where measured spectrum does not follow the model well (such as this), the weighting scheme significantly affects the DSD estimates. We note, however, that in this event, the uniform weight gives better agreements of DSDs with disdrometer data. An example of DSD comparison is given in Fig.4. More study is necessary about the use of this type of weighting.

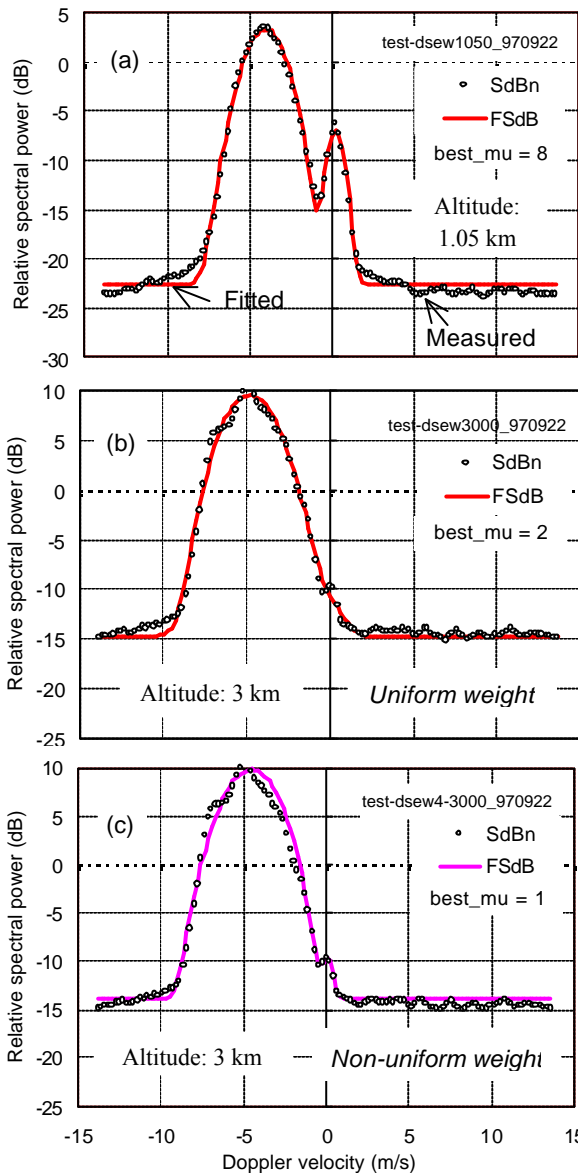


Fig.1(a),(b),(c). Example of LAWP Doppler spectrum fitting. Sep. 22, 1997, Gadanki.

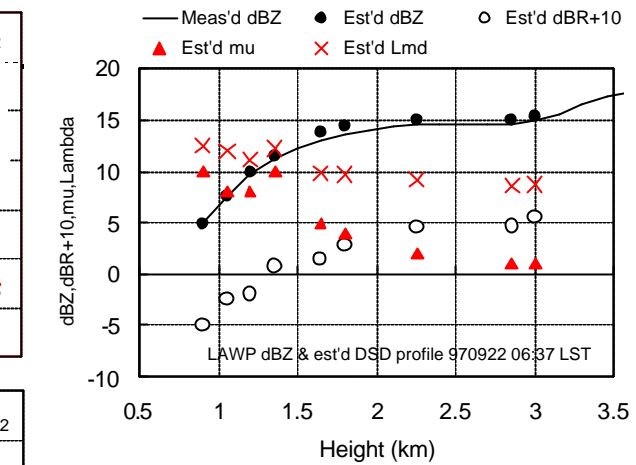
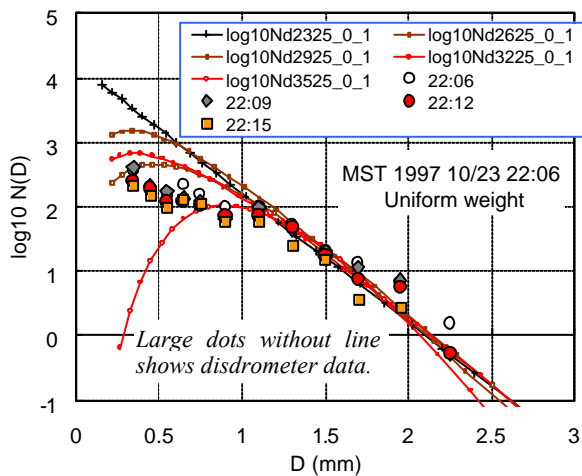


Fig.2. Example of LAWP-estimated DSD parameter profile.

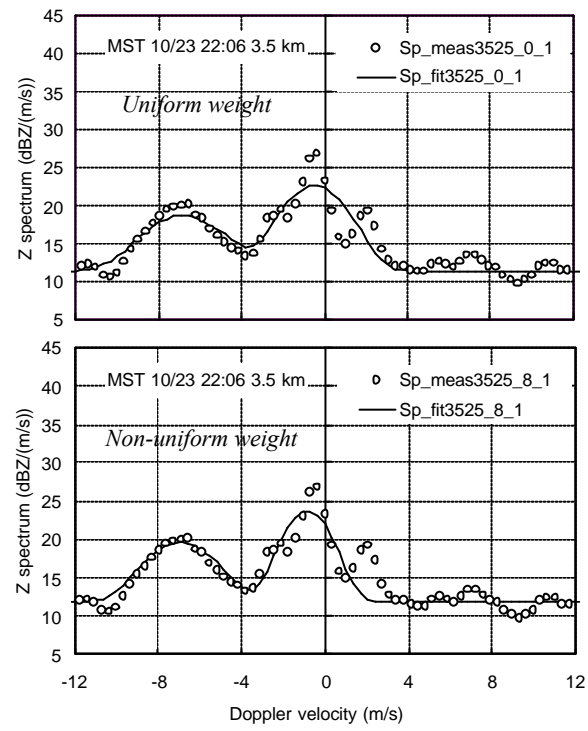


Fig.3. Example of measured and fitted MST radar Doppler spectrum. Oct. 23, 1997, Gadanki.

Fig.4. Example of MST radar estimated DSDs at several heights compared with disdrometer data.

**6.3 DSD estimation with EAR**

The transmit power of EAR is about 1/20 of the MST radar, so the sensitivity to rain is limited. In this paper, we present the analysis of a convective rain around 3-4 LST, March 28, 2002. Fig. 5 shows the comparison of early and "trailing" stages of DSD profiles, compared with disdrometer data. A problem of wind-profiler-based DSD estimation is we have to

assume a fixed  $D-v(D)$  relation. Since particles aloft may not be raindrops, DSD estimates above 0-degree height need to be evaluated carefully. In some cases, discrimination between turbulence and precipitation spectra may be difficult.

Although such caution is needed, we can see some different features in the two sets of vertical DSD profiles. In that the early stage (a), DSDs seem to change slightly from broad to narrow ones, suggesting large initial ice particles aloft, and some break-up & evaporation. In the latter (b), opposite features can be seen. More analyses of raindrop forming processes in this event are necessary.

### 7. Concluding remarks

Case studies of wind profiler based DSD estimation in tropical rainfall were presented. Since disdrometer data analyses have shown much seasonal and climatological dependences of DSD in Asian monsoon regions (Kozu *et al.*, 2001), we are also interested in vertical DSD profiles to get more insight into the micro-physical processes and their relation to larger-scale rainfall properties, which in turn will be connected to the improvement of physical and statistical models of DSD in tropics. Since the EAR site is now equipped with various instruments including an X-band rain radar and a video disdrometer, so that detailed studies on microphysics and rain structures have become possible.

### Acknowledgments

We thank NMRF, India, and CRL, Japan, for providing the MST radar and LAWLP data. The Sumatra project is conducted by a close collaboration with LAPAN, Indonesia. Koto Tabang RD-69 data were provided from Dr. Mori, FORSGC. This work has been partly supported by CREST of JST (Japan Science and Technology Corporation) and by NASDA (National Space Development).

### References

Fukao, S., *et al.*, 2002: Equatorial Atmosphere Radar: System and first results, *Abstracts of International Symposium on Equatorial Processes Including Coupling (EPIC)*, 24, Kyoto, Japan, March 18-22.

Gossard, E. E., 1988: Measuring drop-size distribution in clouds with a clear-air-sensing Doppler radar, *J. Atmos. Ocean. Tech.*, **5**, 640-649.

Kozu, T., *et al.*, 1998: Consideration of raindrop size distribution modeling for wind profiler measurements of precipitation, *Proc. of the Eighth workshop on Technical & Scientific Aspects of MST Radar*, 80-83, Dec 1997.

Kozu, T. *et al.*, 2001: Seasonal variation of raindrop size distribution in south India obtained from disdrometer measurements supported by wind-profiler measurements. *30th Int'l Conf. on Radar Meteorol.*, 7A.6.

Reddy, K.K., *et al.*, 2002: Planetary boundary layer and precipitation studies using lower atmospheric wind profiler over tropical India, *Radio Sci.*, **37**, (4), 14-1 -14-17.

Sato T., *et al.*, 1990: Computer processing for deriving drop-size distributions and vertical air velocities from VHF Doppler radar spectra, *Radio Sci.*, **25**, 961-973.

Wakasugi, K., *et al.*, 1987: Further discussion on deriving drop-size distributions and vertical air velocities directly from VHF Doppler radar spectra, *J. Atmos. Ocean. Tech.*,

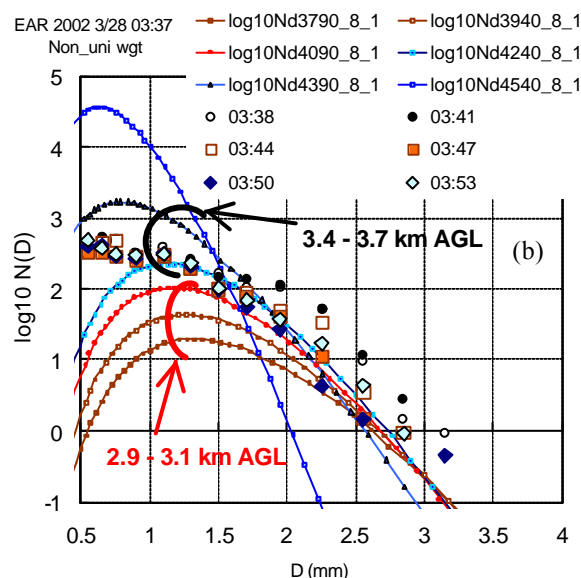
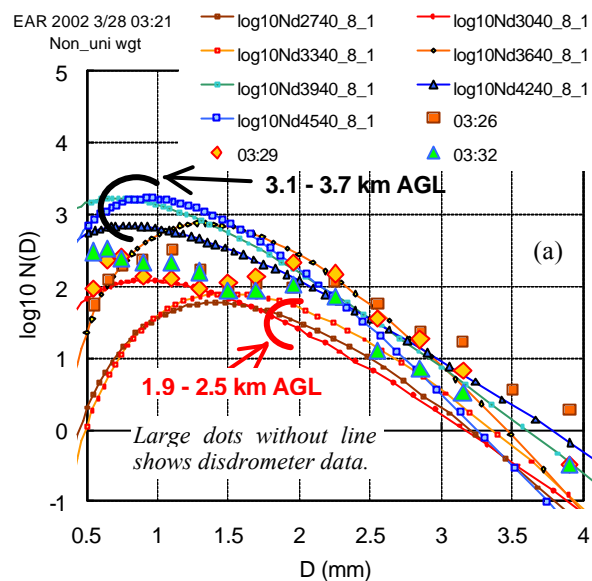


Fig.5. Examples of EAR estimated DSD profiles compared with disdrometer data.